Supporting Information for:

Integrin β1 activation by micro-scale curvature promotes pro-angiogenic secretion of human mesenchymal stem cells

Zhengdong Li, ‡[ab] Weiwei Wang,‡[a] Xun Xu,‡[ab] Karl Kratz,[ac] Jie Zou,[ab] Liudmila Lysyakova,[ac] Matthias Heuchel,[a] Andreas Kurtz,[d] Manfred Gossen,[a] Nan Ma*[abc] and Andreas Lendlein*[abc]

[a] Institute of Biomaterial Science and Berlin-Brandenburg Center for Regenerative Therapies, Helmholtz-Zentrum Geesthacht, Kantstraße 55, 14513 Teltow, Germany; E-mail: nan.ma@hzg.de, andreas.lendlein@hzg.de

[b] Institute of Chemistry and Biochemistry, Freie Universität Berlin, Takustraße 3, 14195 Berlin, Germany

[c] Helmholtz Virtual Institute „Multifunctional Biomaterials for Medicine“, Kantstraße 55, 14513 Teltow, Germany

[d] Charité – University Medicine Berlin, Augustenburger Platz 1, 13353 Berlin, Germany

‡ These authors contributed equally to this work.

Supporting methods

Supporting method S1: surface microscale roughness characterization via optical profilometry

The microscale roughness of the insert bottom was determined with an optical profilometer type MicoProf 200 (FRT - Fries Research & Technologie GmbH, Bergisch Gladbach, Germany) equipped with a CWL 300 μm chromatic white-light sensor. A scan size of 7 x 7 mm^2 was investigated for calculation of the arithmetic average roughness (R_a). The data were acquired

with the software AQUIRE (ver. 1.21) and evaluated with the software MARK III (ver. 3.9). The mean spacing between the peaks (S_m)-value was measured based on the obtained profilometry images. In brief, a mean line was first created and then the average value of the width of peaks at mean line was calculated. The side-view profile of the material surfaces was smoothed by a median filter to eliminate noise with abnormal amplitude.

Supporting method S2: nanotopography and local mechanical analysis by AFM investigations

Surface nanotopography investigations were carried out using an atomic force microscope (AFM, MFP-3D, Asylum Research, Santa Barbara, CA, USA). AC-mode scanning was conducted with a silicon cantilever type OMCL-AC160TS-R3 (Olympus, Tokyo, Japan) having a spring constant of 9 N/m. For topographical analysis an area with a scan size of 2 x 2 μm^2 at three different locations of each sample was investigated in dry state at ambient temperature with a scan rate of 0.5 Hz. The arithmetic average roughness (R_a) of each image was obtained by the commercial software Igor Pro 6.22A and the mean R_a value and the respective standard deviation were calculated from these results.

Nanoindentation measurements were conducted with same instrument (MFP-3D-BIO-AFM, Asylum Research, Santa Barbara, CA, USA) in the dry state at ambient conditions. The used indenter, chosen from the NanoIndenter module (Asylum Research, Santa Barbara, CA, USA), was a standard diamond Berkovich-tip with a spring constant k = 488 N/m, Poisson's ratio of $\nu_{ind} = 0.2$ and Young's modulus of $E_{indenter} = 865$ GPa. For each sample up to 100 single indents were recorded within the whole area of a sample, supported by up to three 64-indent arrays (force maps) in a quadratic area of 90 × 90 μm^2 with an indentation/scan rate of 0.1 Hz and a trigger force of 100 µN. The Young's modulus was calculated by the Oliver-Pharr model [1] in a range from 20% to 90% at the force-distance curve. To determine the mean values, statistical distributions of Young's moduli were fitted using a Gaussian function. Correspondingly, the error bars are represented by the distribution half width. For rough samples (PS-160 and PS-320) the local mechanics were solely analyzed on the "hills" of the microstructures, where an orthogonal indentation can be expected. The calculated mean values of the Young's modulus are listed in Table S1.

Supporting method S3: cell proliferation assay

1.0×10^4 hADSCs were seeded into each insert and the culture medium was changed every 3 days. The number of cells at different time points was determined using a Cell Counting Kit-8 (CCK-8, Dojindo Molecular Technologies, Munich, Germany). In brief, for each insert the old medium was replaced with 300 µl of fresh medium, followed by adding 30 µl of CCK-8 solution. After 3 h of incubation at 37 ºC, 100 µl of medium/CCK-8 mixture were transferred from each insert into a transparent 96-well tissue culture plate, and the absorbance was measured at a wavelength of 450 nm and a reference wavelength of 650 nm using a microplate reader (Infinite 200 PRO, Tecan Group Ltd., Männedorf, Switzerland). A standard curve, which was generated by measuring the absorbance of a series of samples with known cell numbers, was used to calculate the number of hADSCs in the inserts.

Supporting method S4: cell active integrin and pFAK immunofluorescence staining

After 4 days and 14 days, the cells were fixed with 4% (w/v) paraformaldehyde for 20 minutes, permeabilized with 0.1% (w/v) Triton X-100 for 10 minutes and blocked with 1% (w/v) BSA for 30 minutes. Active integrin ß1 was stained with monoclonal mouse anti-human integrin beta-1 antibody (HUTS-4, Millipore, Darmstadt, Germany) and Alexa Fluor® 488 labeled IgG antibody (Life Technologies, Darmstadt, Germany). pFAK was stained with rabbit anti human phospho-FAK(Y397) antibody (Cell Signaling Technology, MA, USA) and Alexa Fluor® 488 labeled IgG antibody (Life Technologies, Darmstadt, Germany). F-actin was stained with Alexa Fluor® 555 Phalloidin (Life Technologies, Darmstadt, Germany). The cell nuclei were stained with Hoechst 33342 (NucBlue® Live Reagent, Life Technologies, Darmstadt, Germany). After staining, the samples were scanned with a confocal laser scanning microscope (LSM 780, Carl Zeiss, Jena, Germany) and the images were processed with ZEN 2012 software (Carl Zeiss, Jena, Germany).

Supporting method S5: Western blotting

Cell lysates from the hADSCs at day 4 and day 14 were prepared with RIPA buffer (Sigma-Aldrich, St. Louis, MO, USA) supplemented with phenylmethylsulfonyl fluoride (Life Technologies, Darmstadt, Germany) and Protease Inhibitor Cocktails (Sigma-Aldrich, St. Louis, MO, USA). After centrifugation, the supernatant of cell lysates was stored at -80 ºC. To quantify

the integrin and FAK expression, the protein solutions were denatured by heating at 95 °C for 5 minutes, separated by electrophoresis on 4–20% Mini-PROTEAN ® TGX™ Precast Protein Gels (Bio-Rad, München, Germany) and then transferred onto nitrocellulose membranes (Millipore, Darmstadt, Germany). The blots were probed with monoclonal primary antibodies (mouse anti-human integrin beta-1 antibody (HUTS-4, Millipore, Darmstadt, Germany), rabbit anti human total integrin beta-1 antibody (Abcam, Cambridge, UK) or mouse anti human FAK antibody and rabbit anti human phosphor-FAK(Y397) antibody (Cell Signaling Technology, MA, USA)) and the IRDye 680LT and IRDye 800CW secondary antibodies (Li-Cor, Bad Homburg, Germany). Fluorescent signal were then detected using an Odyssey Imaging scanner and the intensity was analyzed by image studio software (Li-Cor, Bad Homburg, Germany).

Supporting method S6: model-based analysis of regulation of micro-roughness on hADSCs

To investigate the complex relation between surface roughness, local curvature, and cell development, the optical profilometry experiments on the PS surface samples PS-160 and PS-320 were further analyzed. Fig. S6A and S6B show typical examples for 3D height profiles for samples PS-160 and PS-320 over a base area of 1000 × 1000 μm^2. To determine local surface area values, the base area was divided into 5 × 5 partitions of 200 × 200 μm^2, indicated by the black grids. The 3D height profile of the central partition of the grid (marked in green) is presented enlarged in Fig. S6C for the PS-160, and in Fig. S6D for the PS-320 sample. Image analysis determines for the PS-160 partition a surface area A of 47085 μm^2 and for the PS-320 partition a significant larger value of 129400 μm^2. These values should be set in ratio to the surface A_0 of the respective base area (40000 μm^2). A larger local surface area is a result of extent and spatial distribution of local curvature effects. Therefore, the ratio A/A_0 can be used as a (spatial averaged) estimate of surface curvature. For the two partitions, values of the surface area ratio $S_{AR} = A/A_0$ of 1.18 and 3.24 are obtained. Assuming half spherical valleys as local surface structure with $A = 4\pi r^2/2$ and $A_0 = \pi r^2$ a ratio of $S_{AR} = 2.0$ would result as "curvature measure". On the other side a flat surface would be characterized by $S_{AR} = 1.0$. The sample PS-160 with $S_{AR} = 1.18$ shows in the 3D profile Fig. S6C a hilly and well curved structure and is characterized by maximum roughness depth values of about 35 μm. The rougher PS-320 surface (Fig. S6D) with $S_{AR} = 3.24$ shows a canyon structure with plateaus and deeply incised valleys (profile depth about 190 μm). Here the flat walls of both sides of the valleys contribute

significantly to the high local surface area, but not to a curvature of the surface. From the presented image analysis, one can conclude that S_{AR} values between 1.10 and 2.0 should characterize well curved surfaces in the respective surface level. The lower value was chosen to distinguish from "real" flat surfaces, which show always some small roughness. Assuming a diameter of 100 µm for the living cells, the selected base areas with a side length of 200 µm are in the same size level as the cells, because a respective square could accommodate up to 4 or 5 cells. So, finally one can use the S_{AR} parameter to estimate the extent of surface regions of a sample, where an optimal curvature for cell growing can be expected. Fig. S6E and S6F show for the two polymer samples PS-160 and PS-320 the 2D distribution of S_{AR} values over the 25 partitions of the grid over the 3D height profiles of Fig. S6A and S6B. The PS-160 sample (Fig. S6E) contains extended regions of "optimal" S_{AR} values, indicated in green. They are surrounded by more or less flat regions with only low surface curvature ($S_{AR} < 1.1$). The PS-320 sample (Fig. S6F) shows a significantly smaller proportion of "green region", i.e. optimal for cell growth. The surface of the PS-320 sample is dominated through the central canyon region with a high surface area ratio, $S_{AR} > 2.0$, indicated in light gray, and two "flat" regions ($S_{AR} < 1.1$), which are also significant in extension.

Supporting tables, figures and legends

Supporting Table S1. Surface roughness and local mechanics characterization

Sample ID	Micro-roughness [a]		Nano-roughness [b]	Local mechanics [c]
	R_a (µm)	S_m (µm)	R_a (nm)	Young´s modulus (GPa)
PS-000	0.13 ± 0.07	/	2.6 ± 0.8	31 ± 2
PS-160	4.17 ± 0.17	164 ± 16	12.0 ± 4.3	30 ± 5
PS-320	25.4 ± 3.8	316 ± 36	7.2 ± 0.4	29 ± 2

[a] Optical profilometry measurement by scanning an area of 7 × 7 mm^2.

[b] Atomic force microscopy experiments with a scan size of 2 × 2 μm^2.

[c] AFM nanoindentation experiments.

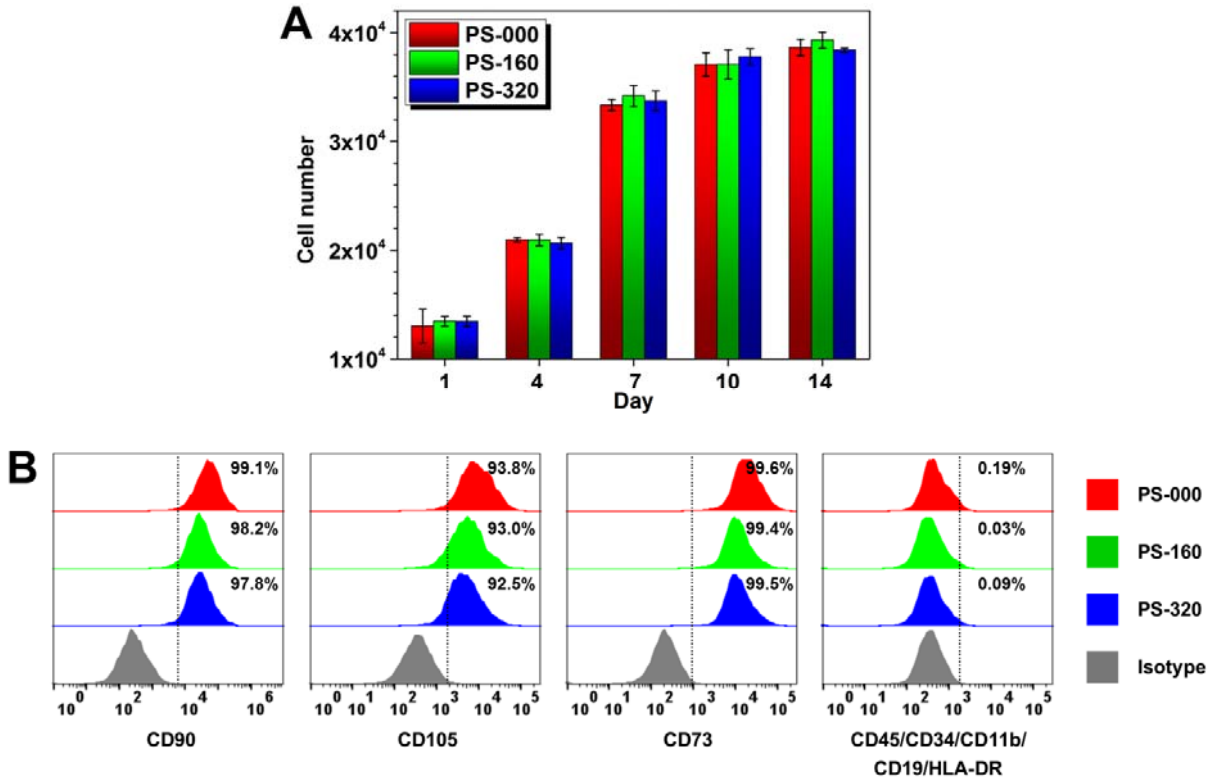

Supporting Fig. S1. Micro-scale surface roughness did not alter hADSC surface markers and proliferation. (A) hADSCs growing on different surfaces exhibited the similar proliferation rate (n = 3). (B) The phenotypic markers of MSCs (CD90, CD105 and CD73) were preserved, and the non-MSC markers (CD45, CD34, CD11b, CD19 and HLA-DR) were negative after 14 days of culture on different surfaces.

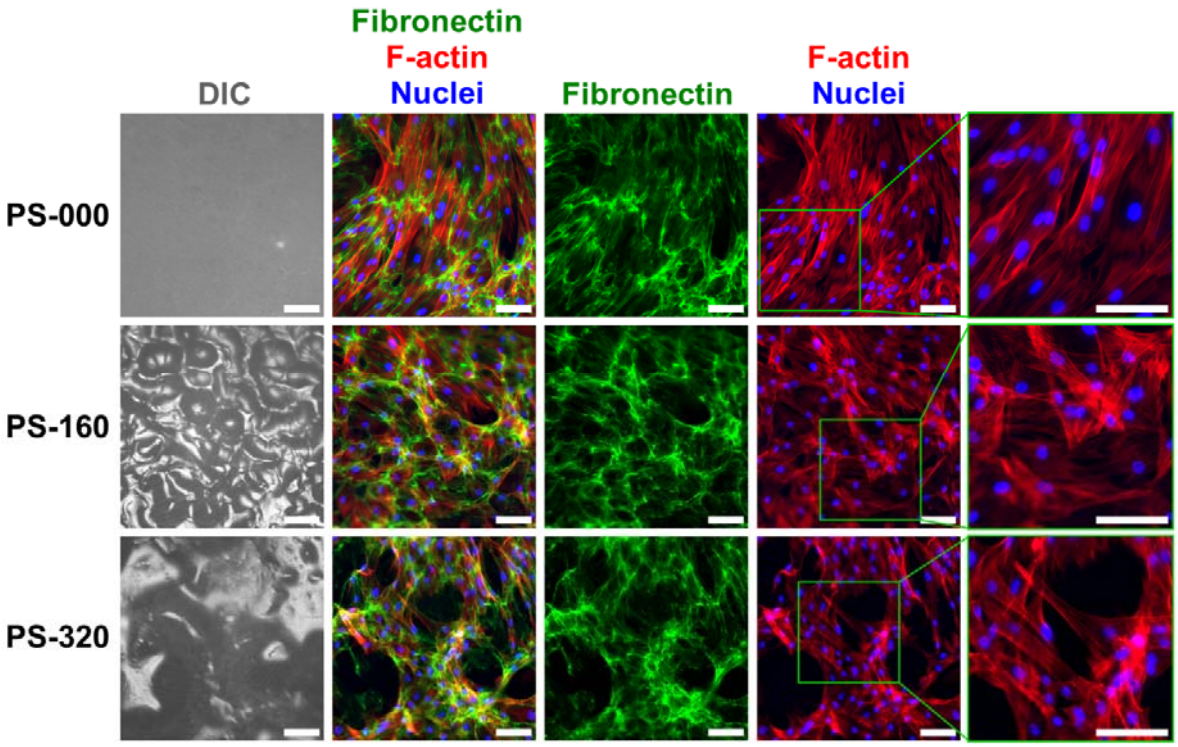

Supporting Fig. S2. The morphology of hADSCs and fibronectin remodeling were influenced by micro-scale roughness. The cells were cultured on fibronectin-coated surfaces followed by fluorescence staining after 4 days of culture to detect the actin cytoskeleton (red), nuclei (blue) and fibronectin (green) using a confocal laser scanning microscope (bar = 100 μm).

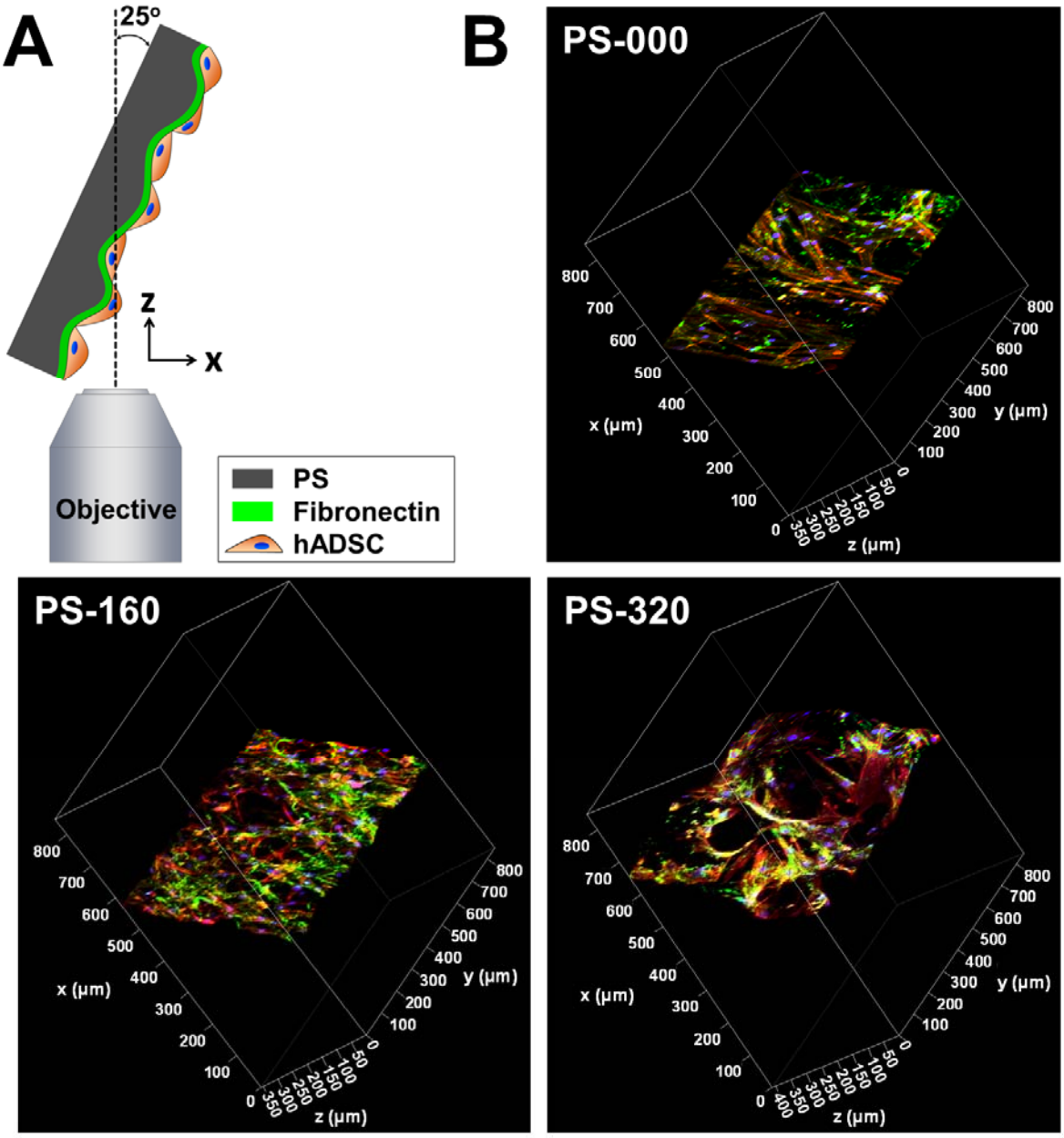

Supporting Fig. S3. 3D reconstruction of tilted-view images of hADSCs cultured on surfaces with different micro-roughness. (A) The scanning was performed by tilting the samples to make a 25° angle between the optical axis of the objective and the material surface. (B) The 3D reconstruction images demonstrated the dominant effect of surface roughness on topography of the cell layers (F-actin: red; nuclei: blue; fibronectin: green).

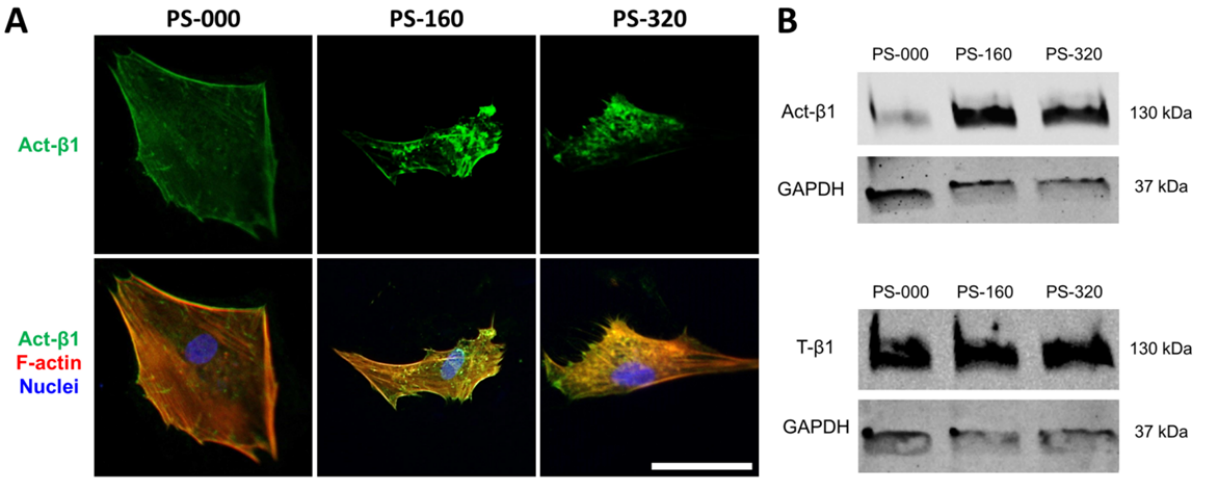

Supporting Fig. S4. Activated and total β1 integrin expression level of hADSCs cultured on different substrates for 4 days: (A) Immunostaining of activated β1 integrin (green) F-actin (red) and cell nuclei (blue) (bar = 50 μm); (B) Representative images of Western blot analysis of activated and total β1 integrin of hADSCs on different substrates.

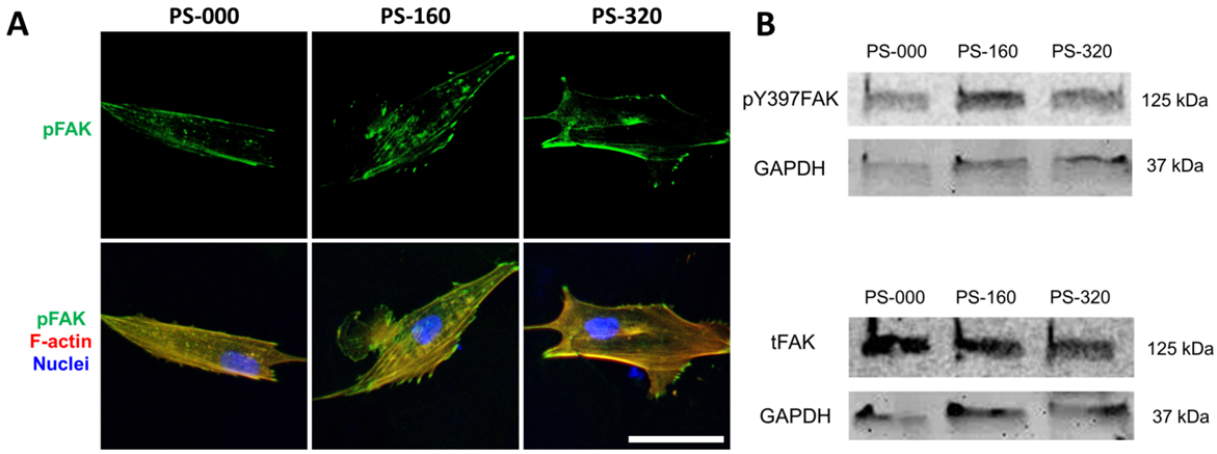

Supporting Fig. S5. Level of phosphorylated FAK in hADSCs cultured on different substrates for 14 days: (A) Immunostaining of phosphorylated FAK (green) F-actin (red) and cell nuclei (blue) (bar = 50 μm); (B) Representative images of Western blot analysis of phosphorylated FAK at Y397 and total FAK.

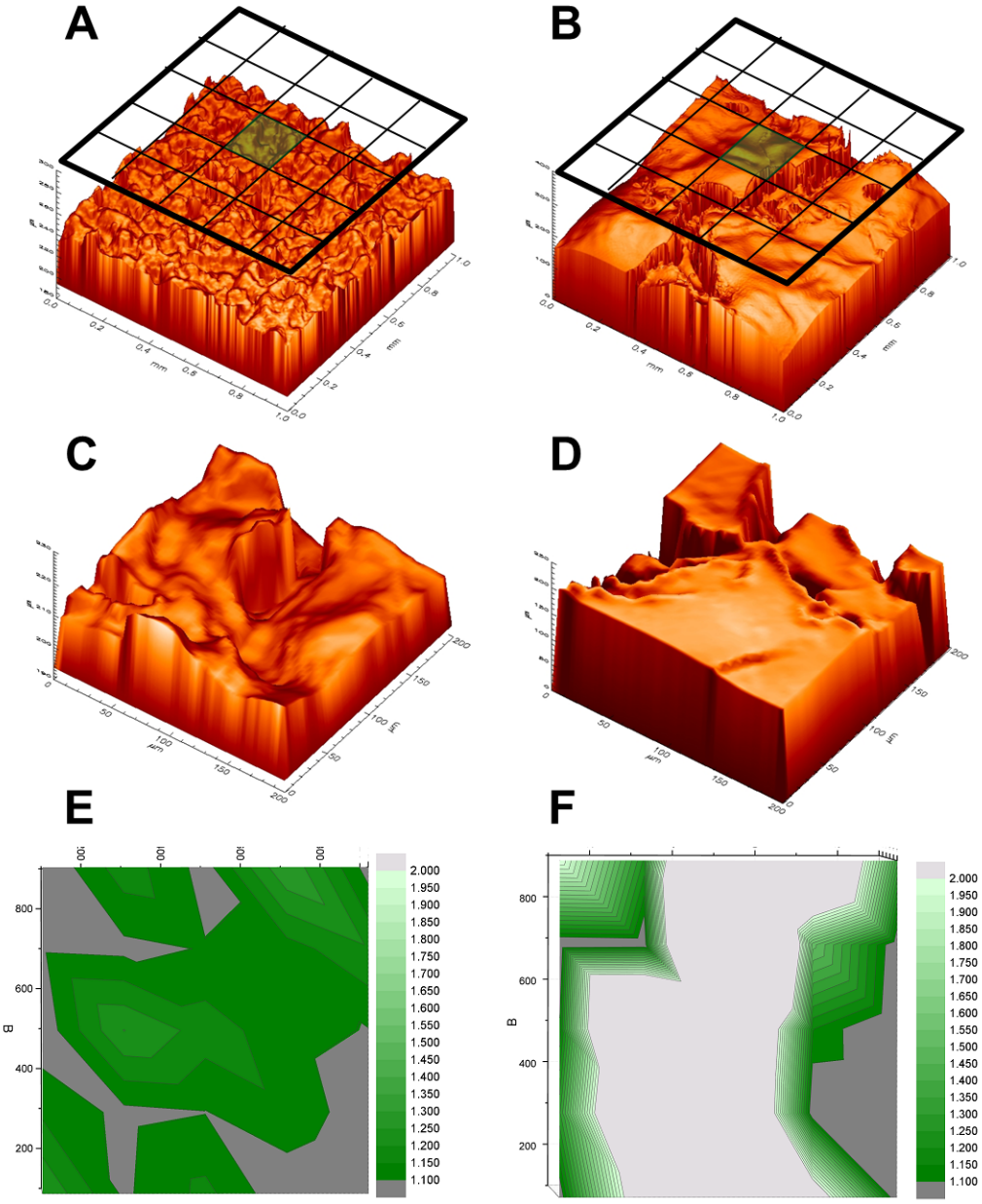

Supporting Fig. S6. Model-based analysis of the optical topography measuring data for the two polymer samples PS-160 (left) and PS-320 (right). 3D height profiles over a base area of 1000 × 1000 µm^2 for samples PS-160 (A) and PS-320 (B). To access local surface area values, the base area was divided into 5 × 5 partitions of 200 × 200 µm^2, indicated by the black grid. 3D height profile of the central partition of the grid (marked in green) is enlarged for PS-160 (C) and PS-320 (D). The 2D distribution of the surface area ratio parameter $S_{AR} = A/A_0$, calculated for the 25 partitions of the grid over the surface, are presented for samples PS-160 (E) and PS-320 (F).

Supporting references

[1] W.C. Oliver and G.M. Pharr, Measurement of Hardness and Elastic Modulus by Instrumented Indentation: Advances in Understanding and Refinements to Methodology, J. Mater. Res. 2004, 19, 13-20.

[2] Xu X, Wang WW, Kratz K, Fang L, Li ZD, Kurtz A, et al. Controlling Major Cellular Processes of Human Mesenchymal Stem Cells using Microwell Structures. Adv. Healthcare Mater. 2014,3,1991-2003.